Mechanical and Thermal Properties of Poly(butylene succinate)/Plant Fiber Biodegradable Composite

Zhichao Liang, Pengju Pan, Bo Zhu, Tungalag Dong, Yoshio Inoue

Department of Biomolecular Engineering, Tokyo Institute of Technology, Nagatsuta, Midori-ku, Yokohama 226-8501, Japan

Received 3 September 2008; accepted 6 December 2008
DOI 10.1002/app.29848
Published online 4 November 2009 in Wiley InterScience (www.interscience.wiley.com).

ABSTRACT: Biodegradable polymeric composites were fabricated from poly(butylene succinate) (PBS) and kenaf fiber (KF) by melt mixing technique. The mechanical and dynamic mechanical properties, morphology and crystallization behavior were investigated for PBS/KF composites with different KF contents (0, 10, 20, and 30 wt %). The tensile modulus, storage modulus and the crystallization rate of PBS in the composites were all efficiently enhanced. With the incorporation of 30% KF, the tensile modulus and storage modulus (at 40°C) of the PBS/KF composite were increased by 53 and 154%, respectively, the crystallization temperature in cooling process at 10°C/min from the melt was increased from 76.3 to 87.7°C, and the half-time of PBS/KF composite in isothermal crystallization at 96 and 100°C were reduced to 10.8% and 14.3% of that of the neat PBS, respectively. SEM analysis indicates that the adhesion between PBS and KF needs further improvement. These results signify that KF is efficient in improving the tensile modulus, storage modulus and the crystallization rate of PBS. Hence, this study provides a good option for preparing economical biodegradable composite. © 2009 Wiley Periodicals, Inc. J Appl Polym Sci 115: 3559–3567, 2010

Key words: poly(butylene succinate); (PBS); kenaf fiber; mechanical properties; crystallization behavior

INTRODUCTION

In recent decades, research on the application of natural fibers as the reinforcement in polymeric composites has attracted increasing interest.[1–4] Natural fiber has advantages of low cost, low density associated with acceptable specific mechanical properties. Especially, its renewability and biodegradability represent the viewpoint of protecting natural environment.[1,4] Therefore, it has been regarded as an economical and ecological potential alternative to the traditional synthetic reinforcement, such as glass fibers and carbon fiber, in polymeric composite.[2,4]

The integration of natural fiber and conventional polyolefins, polystyrene, and epoxy resin in composites, have been extensively studied,[5–15] because of the increasing interest in their applications in various areas, such as automotive industry, furniture industry and leisure industry.[2–16] However, most of the widely used conventional polymers are not biodegradable and induce some environmental problems. Therefore, increasing interest has been attracted in developing environment-friendly composites or biocomposites by reinforcing the biocompatible and biodegradable polymers with the plant-derived fibers.[17–29]

Among the family of environment-friendly biodegradable polymers, aliphatic polyesters have attracted increasing attention because of their biocompatibility and biodegradability.[3,4] With a good flexibility characterized by high fracture strain, the commercialized poly(butylene succinate) (PBS) is a high potential choice among the aliphatic polyesters. However, the modulus of PBS is relatively low, typically 300–500 MPa, and its price is much higher than the traditional thermoplastics. These drawbacks may have some limitation in its commercial application. A solution for this problem is fabricating the biodegradable composites of PBS with natural fiber as the reinforcement. One of the natural fibers is the bamboo fiber, but it has been reported that the glyoxal modified bamboo fibers did not show significant improvement on either mechanical properties or crystallization of PBS.[28] Pan et al. have reported that kenaf fiber shows a considerable effect of enhancement in mechanical properties and crystallization on poly(L-lactide)[17] and poly(ε-caprolactone).[18] Therefore, it is considered that reinforcing PBS with kenaf fiber is possibly an efficient way to enhance its mechanical property, and to lower the price of PBS-based materials. Such a composite can be a good option as the economical and biodegradable composite. Moreover, polymer crystallinity plays an

Correspondence to: Y. Inoue (inoue.y.af@m.titech.ac.jp).

important role in the biodegradability of aliphatic polyester,[30] as well as their mechanical and thermal properties. Usually, with increased crystallinity, biodegradability decreases, mechanical properties, especially tensile strength and modulus, and thermal properties are enhanced. However, few of systematic research referring to the effect of the incorporated natural fiber on the crystallization of PBS are reported. Therefore, for optimizing the processing conditions and properties of the final product, it is important to study the effect of KF on the crystallization of PBS, as well as its effect on the mechanical properties of PBS/KF composites.

In present work, the green composites from KF and PBS were fabricated by the melt-mixing technique, and the effect of fiber weight contents on mechanical and dynamical mechanical thermal properties, the nonisothermal and isothermal crystallization behavior were systematically investigated. Moreover, to study the influence of KF on the crystallization process of PBS, the isothermal crystallization kinetics and the spherulite morphology of KF-reinforced PBS composite with different KF contents were also analyzed.

EXPERIMENTAL

Materials

PBS ($M_n = 5.2 \times 10^4$, $M_w/M_n = 1.7$) was purchased from Showa Highpolymer Co. Ltd., Japan. Kenaf fiber (average length = 3 mm, average diameter = 25 μm, specific gravity = 1.48) was kindly supplied by the Nano Electronics Research Laboratories, NEC, Japan.

Composite fabrication

The two components for mixing, PBS and KF, were dried under vacuum at 40°C for 48 h, before the fabricating process. The composites were prepared by extruding the polymer and fiber after mixing them in a single screw machine (Imoto machinery, Kyoto, Japan) with a speed of 100 rpm at 150°C for 2 min. To obtain the desired film samples for various measurements, the composite was hot-pressed with a pressure of 10 MPa after melting at 150°C for 2 min, before being quenched to 25°C under room conditions. The samples are denoted as PBS/KF (x/y), where x and y represent the weight percentages of PBS and KF, respectively.

Measurements

Tensile test

Tensile properties were investigated with the EZ test machine (Shimadzu, Kyoto, Japan) at a crosshead speed of 5 mm/min. All samples have a gauge length of 22.5 mm, width of 4.76 mm, and a thickness of about 0.37 mm. Each value of mechanical properties reported here was an average of seven specimens.

Dynamic mechanical thermal analysis

The samples of composites were thin rectangular strips with dimensions of 30 × 10 × 0.37 mm^3. The storage modulus (E'), loss modulus (E''), and loss factor (tanδ) of the pure PBS and the composites were measured as a function of temperature (−70 to 130°C) with the aid of a DMS210 (Seiko Instrument, Japan) equipped with SSC5300 controller at a frequency of 5 Hz and a constant heating rate of 2°C/min.

Scanning electron microscopy

The morphology of KF and the fractured surface of neat PBS and the PBS/KF composites were evaluated with a scanning electron microscope model JSM-5200 (JEOL, Tokyo, Japan). Before the surface characterization, the samples were coated with gold particles up to thickness of about 10 nm.

Thermogravimetric analysis

A TG/DTA 220U with the Exstar 6000 Station (Seiko Instrument, Tokyo, Japan) was used for thermogravimetric analysis (TGA) on KF, neat PBS and the PBS/KF composites. The samples were scanned from 30 to 600°C at a heating rate of 5°C/min in the presence of nitrogen flow.

Differential scanning calorimeter

The crystallization behavior of the neat PBS and PBS/KF composites were analyzed with a Pyris Diamond Differential scanning calorimeter (DSC) instrument (Perkin–Elmer Japan, Yokohama, Japan). The scales of temperature and heat flow at different heating rates were calibrated using an indium standard. The samples were weighted and sealed in an aluminum pan. In the nonisothermal melt-crystallization, the melted samples were cooled to −50°C at a cooling rate of 10°C/min after melting at 150°C for 2 min. Subsequently, the crystallized sample was heated to 150°C at 10°C/min to evaluate the melting behavior. In the isothermal melt-crystallization, the sample melted at 150°C for 2 min was cooled at a rate of 100°C/min to the desired crystallization temperature (T_c) and allowed to crystallize.

Polarizing optical microscopy

The spherulite morphology of the pure PBS and the PBS/KF composites was observed on an Olympus

TABLE I
Tensile Properties of Neat PBS and PBS/KF Composites

Sample	Tensile strength (MPa)	Tensile modulus (MPa)	Fracture strain (%)
PBS	33.5 ± 1.7	434 ± 21	213 ± 11
PBS/KF (90/10)	18.9 ± 1.0	469 ± 24	10 ± 0.5
PBS/KF (80/20)	19.1 ± 1.0	578 ± 29	7 ± 0.4
PBS/KF (70/30)	18.6 ± 0.9	664 ± 34	5 ± 0.3

BX90 polarizing optical microscopy (POM) (Olympus, Tokyo, Japan) equipped with a digital camera. The sample was placed between a microscope glass slide and a cover slip, and the temperature was controlled by a Mettler FP82 HT hot stage. The sample was at first heated to 150°C and held for 2 min before it was quenched to 96 and 100°C for isothermal crystallization. The spherulite morphology was recorded by taking microphotographs after the crystallization finished.

Wide-angle X-ray diffraction

A Rigaku RU-200 (Rigaku, Tokyo, Japan) was used for wide-angle X-ray diffraction (WAXD) analysis on the neat PBS and PBS/KF composites, working at 40 kV and 200 mA, with Ni-filtered Cu Kα radiation (λ = 0.15418 nm). Scans were made between Bragg angles of 5–50° at a scanning rate of 2°/min.

RESULTS AND DISCUSSION

Tensile properties

The tensile strength, modulus, and fracture strain of neat PBS and PBS/KF are summarized in Table I. Table I shows the tensile modulus of neat PBS and its composites with different content of KF. The neat PBS has a tensile strength of 33.5 MPa, a modulus of 434 MPa, and a fracture strain of 213%. As shown in Table I, the incorporation of KF improved the tensile modulus of PBS, indicating that transferring of stress from the polymer matrix to the stiffer fiber occurred. Comparing to the neat PBS, the tensile modulus of the PBS/KF composites containing 20 and 30 wt % of KF increase by 33 and 53%, respectively. However, the tensile strength and the fracture strain of the composites decrease with increasing content of KF. This could be attributed to the less adequate adhesion between KF and PBS, resulting in the poor interfacial interaction and debonding of the matrix from the fiber during the tensile deformation. The debonding results in void formation, which lowers the tensile strength because cracks can easily propagate through regions containing voids.[31]

Generally, the addition of a high amount of fiber can reduce the failure strain. In the composite, all of the elongation arises from the polymer matrix because the KF fiber is rigid relative to PBS. Increasing the amount of filler decreases the amount of polymer available for the elongation.[31] Moreover, adding higher amount of fiber increases the possibility of fiber agglomeration. Such an agglomeration can lead to the formation of stress concentrated region where less energy is required for elongating the crack propagation.[22] During the tensile deformation, the inefficient stress-transfer nearby the stress concentrated region may result in the failure of specimens before the yield.

Dynamic mechanical thermal analysis

Figure 1(a,b) show the dynamic storage modulus (E') and tanδ of the pure PBS and PBS/KF

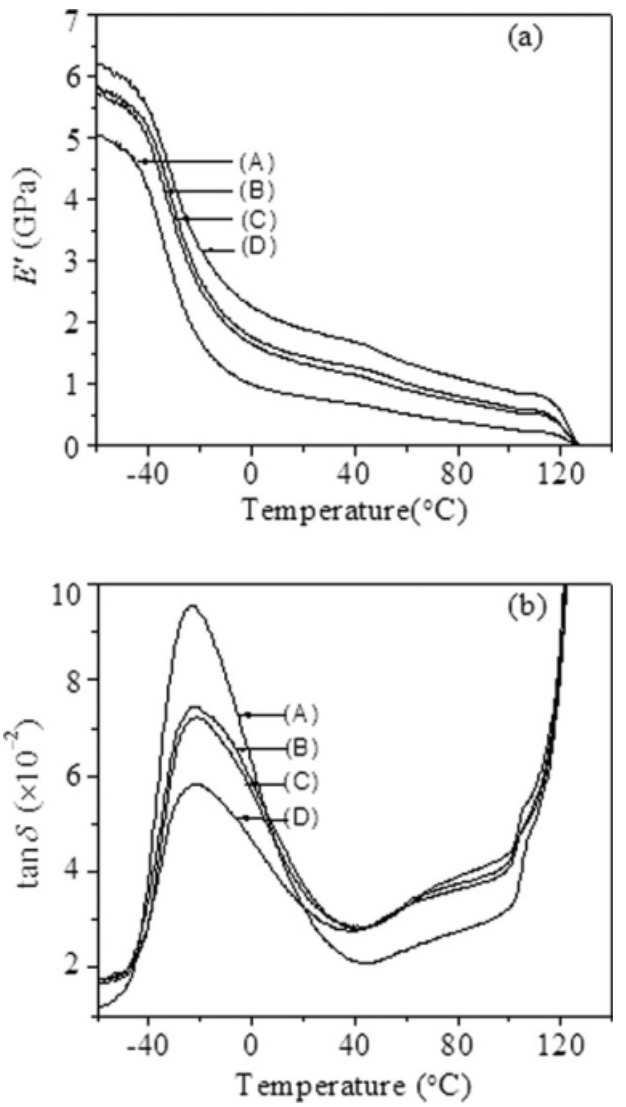

Figure 1 Temperature dependence of (a) storage modulus and (b) tanδ of neat PBS and PBS/KF composites: (A) neat PBS, (B) PBS/KF(90/10), (C) PBS/KF (80/20) and (D) PBS/KF (70/30).

TABLE II
Storage Modulus of Neat PBS and PBS/KF Composites

Sample	E' at −50°C (GPa)	E' at −23°C (GPa)	E' at 0°C (GPa)	E' at 40°C (GPa)
PBS	4.81	1.99	1.01	0.67
PBS/KF(90/10)	5.50	2.82	1.66	1.16
PBS/KF(80/20)	5.62	3.02	1.78	1.30
PBS/KF(70/30)	5.98	3.53	2.27	1.70

composites, respectively, as a function of temperature. As shown in Figure 1(a), with the incorporation of KF, the storage modulus of PBS/KF composites is higher than that of neat PBS. This indicates that the stress transferred from the matrix to the kenaf fiber. As shown in Table II, the E' value of PBS/KF(70/30) at 40°C increased by 154% relative to that of neat PBS. In the composites, the change in modulus from the glassy state to rubbery state is smaller than that in neat PBS. This may be attributed to two reasons, the combination of the hydrodynamic effects of the fibers embedded in a viscoelastic medium and the mechanical restraint introduced by the incorporated filler, which reduced the mobility and deformability of the matrix.[11] Furthermore, the E' value of both PBS and its composites decreased with increasing temperature, due to the softening of the polymer matrix.

As shown in Figure 1(b), the temperature of tanδ peak is about −23°C for all samples. Its height decreased with the addition of KF. The decrease of tan δ peak can be attributed to the decrease of content of PBS in the composites. The damping or tanδ in the transition region measures the imperfections in the elasticity of a polymer.[31] Therefore, with the presence of KF, the molecular mobility of the materials decreases and the mechanical loss to overcome intermolecular chain friction is reduced.[32] In the composites, as the amount of incorporated fiber becomes higher, the contact area between the fiber and the polymer matrix increases, leading to the stronger interfacial interaction between the fiber and matrix. Hence, the chain mobility of PBS around the fiber is restrained, resulting in the improvement in the hysteresis of the system and a reduction in the internal friction.

Morphology of composites

The morphologies of KF, neat PBS and PBS/KF composites were investigated with Scanning electron microscopy (SEM). The SEM micrographs of the KF are shown in Figure 2(a,b), where the diameter and the morphology of KF are revealed. The kenaf fibers have diameters ranging from 5 to 50 μm, with rough surface with some small fibers and particles adhered on. These variations are probably attributed to the different sources and the processing history of the fibers.

SEM micrographs of the tensile-fractured surfaces of the neat PBS and PBS/KF composite are shown in Figure 2(c–f). As shown in Figure 2(c), the tensile-fractured surface of neat PBS is with craze and fibril on the surface, revealing that PBS fractured in the

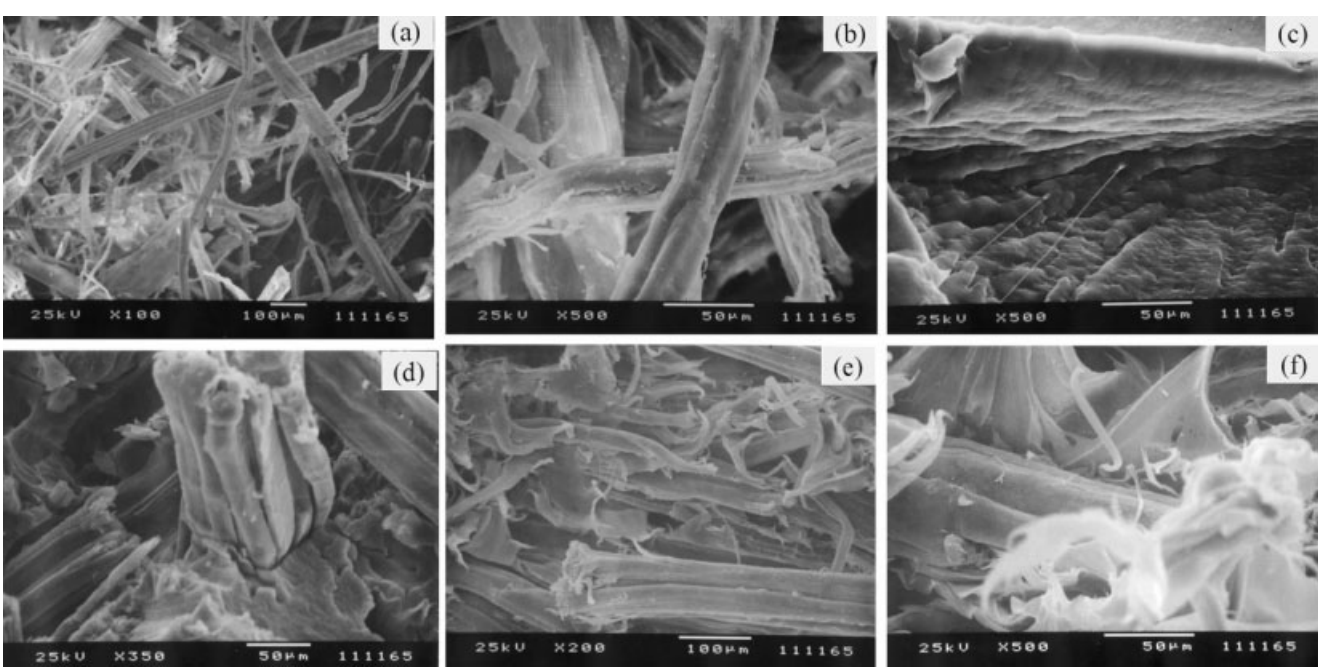

Figure 2 SEM micrographs of (a) ×100 and (b) ×500 kenaf fiber, (c) tensile-fractured surface of neat PBS, (d) frozen-fractured surface of PBS/KF (70/30), (e) ×200 and (f) ×500 tensile-fractured surface of PBS/KF (70/30).

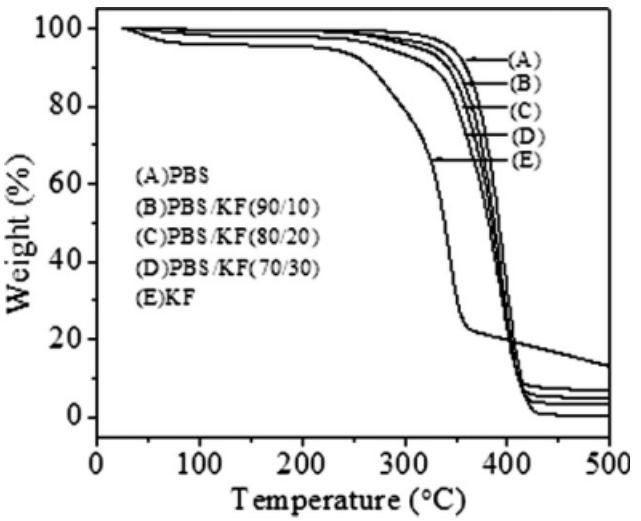

Figure 3 TGA curves of (A) neat PBS, (B) PBS/KF (90/10), (C) PBS/KF (80/20), (D) PBS/KF (70/30), and (E) KF.

"ductile" manner. The fracture surface of frozen-fractured and tensile-fractured PBS/KF(70/30) specimens are depicted in Figure 2(d–f), respectively. As shown in Figure 2(d), the surface of KF is smooth in the composite, and the fibrils linking the fiber surface to the matrix can be observed. Furthermore, in Figure 2(d), the fiber seems to be covered by a thin layer of PBS matrix, but the separation between the fiber and the polymer matrix is also observed. It indicates that the interfacial adhesion between the fiber and the matrix is less adequate. This may lead to deficient stress transfer between the polymer matrix and the reinforcing fiber. As seen in Figure 2(e,f), the fracture surface is irregular and the pull-out fiber is prevailed over the fiber fracture. Additionally, as shown in Figure 2(e), the debonding of the PBS matrix and fiber is observed. These suggest that the interfacial adhesion between fiber and the polymer matrix can be further improved. The mechanical properties of composite greatly depend on the state of the filler dispersion and the strength of the interfacial interaction or adhesion. As reported by Dong et al., the interfacial interaction between bulk polymer and nucleating agent has a significant influence on the crystallization rate.[33] Therefore, it is expected that the mechanical properties as well as the crystallization behavior can be further optimized, if the compatilizers or coupling agents are used to improve the interfacial interaction and the compatibility between the fiber and PBS matrix.

Thermogravimetric analysis

The thermal stability of neat PBS, KF and PBS/KF composites was investigated with TGA. The results are shown in Figure 3. In Table III, the 5%, 25%, 50%, and 75% weight-loss temperatures, which are represented by T_5, T_{25}, T_{50}, and T_{75} respectively, are listed for all the samples shown in Figure 3. As reported in a research by Pan et al., KF degrades by three stages with heating,[17] similar with the decomposition behavior of other plant fibers such as the bamboo fiber and the recycled newspaper fiber.[21,22] The first stage, from 30 to 140°C, is attributed to the release of absorbed moisture in the KF fiber. The second transition, from 140 to 360°C, is due to the degradation of cellulosic substances such as hemicelluloses and cellulose. The third stage, from 360 to 500°C, is related to the degradation of noncellulosic materials in the fiber. As seen in Figure 3, in the second stage, the degradation rate of KF is slow below 250°C, but after 250°C it becomes fast. In third stage, the relationship between weight and temperature is almost linear. The neat PBS shows an onset temperature of thermal degradation around 350°C, which is much higher than that of KF at about 220°C. Therefore, with increased content of KF, the rate of thermal weight-loss of the PBS/KF composites increased, and the onset temperature of thermal degradation of the composites decreased. However, this may not mean that the thermal stability of PBS/KF composites is worse than that of neat PBS. The weight-loss may be attributed to the char yield of the composite, which may limit the production of the pyrolysis reaction and inhibit the thermal conductivity of the burning material.[25] This implies that the incorporation of KF in the composite might increase the thermal stability of the samples.

Nonisothermal crystallization

For neat PBS and PBS/KF composites, DSC curves of the nonisothermal melt-crystallization with a cooling rate of 10°C/min and the subsequent melting with a heating rate of 10°C/min, are presented in Figure 4(a,b), respectively. The thermal properties including the crystallization temperature (T_c), melting peak temperature(T_m), crystallization enthalpy (ΔH_c), melting enthalpy (ΔH_m), all obtained from the DSC analysis, as well as the calculated degree of crystallinity (X_c%), are summarized in Table IV. The degree of crystallinity (X_c%) was calculated from

TABLE III
TGA Characterization of Neat PBS, KF and PBS/KF Composites

Sample	T_5 (°C)	T_{25} (°C)	T_{50} (°C)	T_{75} (°C)
PBS	345	377	392	404
KF	220	310	338	356
PBS/KF(90/10)	330	371	387	400
PBS/KF(80/20)	313	365	385	399
PBS/KF(70/30)	281	357	382	398

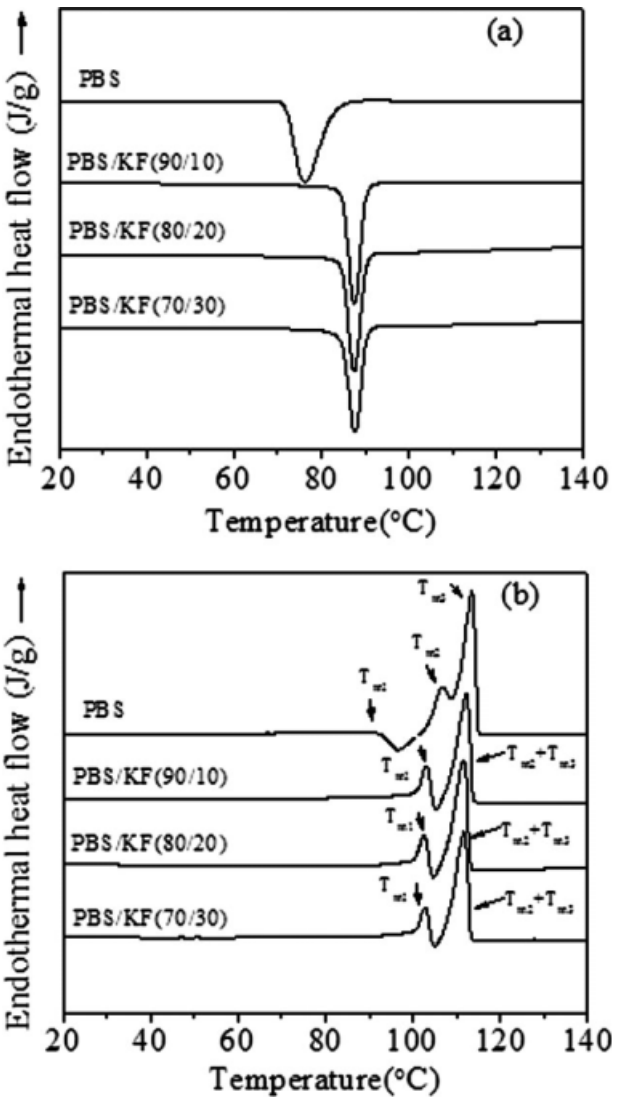

Figure 4 DSC curves of (a) nonisothermal melt-crystallization with cooling rate of 10°C/min and (b) subsequent melting with heating rate of 10°C/min of PBS and its composites with KF.

$\Delta H_m/\Delta H_m^0$, where ΔH_m^0 is the melting enthalpy of the polymer when its crystallinity is 100%. The ΔH_m^0 of PBS has been reported to be 200 J/g.[34] As shown in Figure 4, the neat PBS sample shows a low crystallization temperature (76.3°C) during the cooling process, however, the crystallization peak of PBS shifted to a higher temperature and became sharper with the addition of KF in the composites, demonstrating that the crystallization rate of PBS was enhanced with incorporated KF. In the subsequent heating process, the melting behavior of PBS has a distinct feature that PBS crystals partially melted and recrystallized,[33] as shown in Figure 4(b). T_{m1}, T_{m2}, T_{m3} indicate the melting peaks. The melting peak T_{m3} observed at the highest temperature ($\sim$ 113.6°C) is not dependent to the crystallization in the previous cooling process, but corresponds to the recrystallization of the partially melted crystals during the heating process.[33,35] The T_{m1} and T_{m2} peaks are possibly attributed to the melting of original crystalline.[35] As shown in Figure 4(b), with incorporated KF, PBS in the composites exhibits higher values of T_{m1}, T_{m2} than those of the neat PBS. This indicates the formation of more perfect crystalline phase, corresponding to the higher crystallization temperature of PBS/KF composites in the cooling process.

Generally, the crystallization process in the polymeric composites system is more complicated than that of the neat polymer, because of the impact of the incorporated filler, such as KF in the present work. This process may be mainly controlled by two factors:[21,36] the positive one that the filler has the nucleation effect on the crystallization and thereby enhances the crystallization, and the negative one that the filler hinders the migration and diffusion of polymeric molecular chains to the surface of the growing face of the polymer crystal in the composites.

As seen in Figure 4 and Table IV, the crystallization temperature of PBS was raised dramatically in the presence of small amount of KF. This indicates the significant promotion in the crystallization rate due to the nucleating effect of KF, and results in the increase of crystallinity of PBS in the composites when the KF content is less than 20%. Nevertheless, in the PBS/KF composites, the T_c value was almost not changed with further increase in the KF content. Besides, as presented in Table IV, when the KF content is higher than 20%, the degree of crystallinity of the composites decreased as KF content increased, signifying that the KF fibers may also hinder the migration and diffusion of PBS molecular chain to the surface of the nucleus in the composites, besides the nucleation effect.

Isothermal crystallization

DSC was also used for the investigation on the isothermal crystallization behavior of neat PBS and PBS/KF composites at a series of temperatures from 75 to 105°C. The results at 96 and 100°C are presented in Figure 5(a,b), respectively. From the DSC

TABLE IV
Crystallization and Melting Behavior of Neat PBS and PBS/KF Composites from DSC Analysis

Sample	T_c (°C)	ΔH_c (J/g PBS)	T_m (°C)		ΔH_m (J/g PBS)	X_c (%)
PBS	76.3	−67.1	105.8	113.6	63.8	31.9
PBS/KF(90/10)	87.3	−58.1	103.1	112.2	64.8	32.4
PBS/KF(80/20)	87.5	−69.5	102.6	111.6	70.1	35.1
PBS/KF(70/30)	87.7	−49.2	102.7	111.7	52.6	26.3

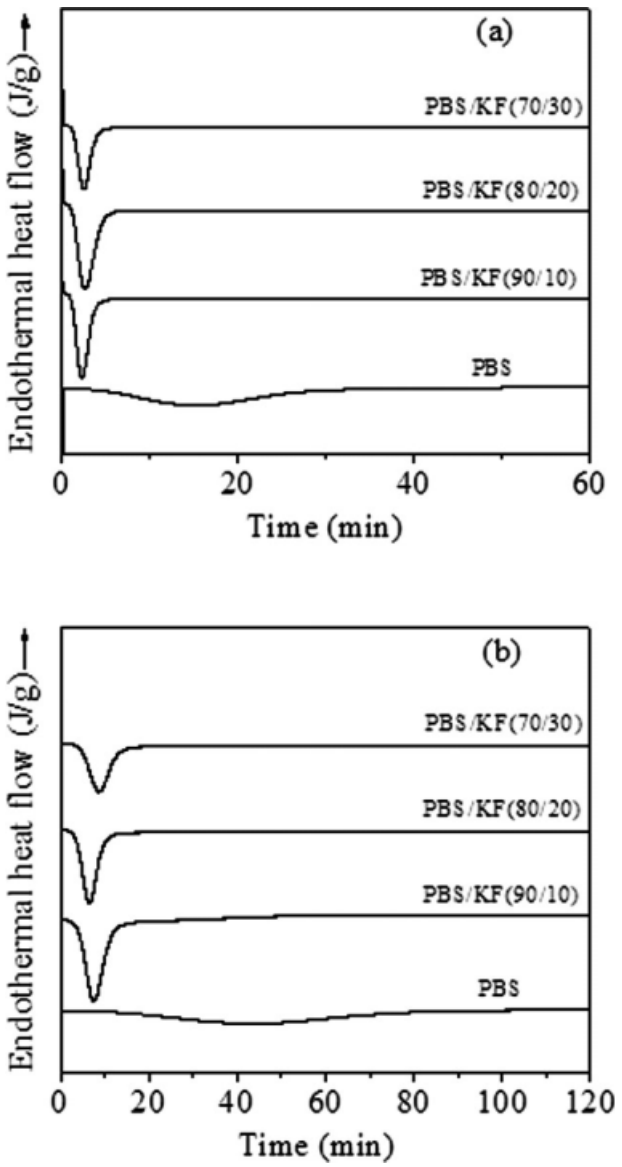

Figure 5 DSC curves of PBS and PBS/KF composites isothermally melt-crystallized at (a) 96 and (b) 100°C.

measurements, the crystallization kinetics was analyzed. The isothermal heat flow curve was investigated to determine the degree of crystallinity of the samples as a function of crystallization time. The relative crystallinity ($X(t)$) at any given time t was calculated from the integrated area of the isothermal heat flow curve from $t = 0$ to $t = t$ divided by that of the whole heat flow curve.

The isothermal bulk crystallization kinetics was analyzed with the Avrami equation:[37,38]

$$X(t) = 1 - \exp(-kt^n) \tag{1}$$

where n is the Avrami index related to the dimensional growth and the way of forming primary nuclei, and k is the overall rate constant associated with both nucleation and growth contributions. The linear form of eq. (1) is given as eq. (2):

$$\log[-\ln(1 - X(t))] = \log k + n \log t \tag{2}$$

The values of n and k are obtained by plotting log[(ln(1($X(t)$))] against log t. Meanwhile, the crystallization half-time $t_{1/2}$, which is defined as the time when the crystallinity arrives at 50%, can be determined from the kinetics parameters measured by using the following equation:

$$t_{1/2} = (\ln 2/k)^{1/n} \tag{3}$$

The crystallization parameters k, n, and $t_{1/2}$ of neat PBS and PBS/KF composites crystallized at 96 and 100°C are listed in Table V. As seen in Figure 5, obviously, the isothermal crystallization rate of PBS in composites is efficiently increased, comparing to that of the neat PBS, signifying that the crystallization of PBS is dramatically enhanced with the addition of KF. This result is also supported by the results of kinetic analysis as listed in Table V. In virtue of the heterogeneous nucleation effect of KF on the crystallization of PBS, the $t_{1/2}$ reduces with the presence of KF. The $t_{1/2}$ values of the PBS/KF(80/20) composite crystallized at 96 and 100°C reduce to 8.9% and 11.7% of the neat PBS, respectively. However, as the KF content in the composite is higher than 20%, the $t_{1/2}$ value increases with the increase of KF content, due to the hindrance of polymer diffusion by KF. The result corresponds well with the results of the nonisothermal DSC analysis. Because of the hindrance of polymer diffusion caused by KF, the crystallization enthalpy of the PBS/KF composites decreases as the KF content increases, when the KF weight content is larger than 20%. Because the more ordered crystal is developed at higher T_c, the

TABLE V
Kinetic Parameters of Neat PBS and PBS/KF Composites Isothermally Melt-Crystallized at 96°C and 100°C

	T_c =96°C				T_c =100°C			
Sample	$t_{1/2}$ (min)	ΔH_c (J/g PBS)	n	log(k)	$t_{1/2}$ (min)	ΔH_c (J/g PBS)	n	log(k)
PBS	15.62	−61.9	2.65	−3.40	38.56	−68.1	2.49	−4.12
PBS/KF(90/10)	1.56	−57.5	2.17	−0.59	7.74	−60.7	2.09	−2.38
PBS/KF(80/20)	1.39	−56.3	2.33	−0.44	4.50	−57.3	2.05	−1.81
PBS/KF(70/30)	1.69	−44.7	2.17	−0.72	5.50	−46.7	2.40	−1.95

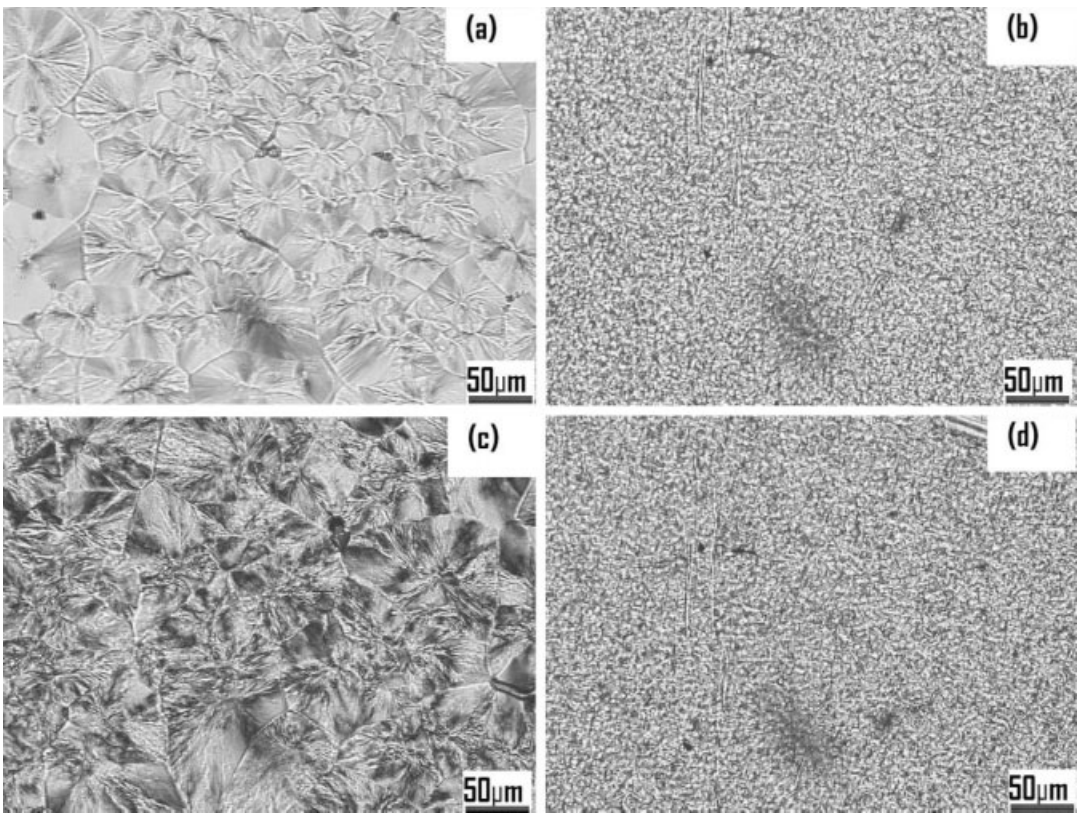

Figure 6 Optical micrographs of (a) and (c) neat PBS, (b) and (d) PBS/KF (90/10) composite isothermally melt-crystallized at (a,b) 96°C and (c,d) 100°C.

crystallization enthalpy of PBS and its composites crystallized at 100°C is larger than that of those crystallized at 96°C.

The spherulite morphology of neat PBS and PBS/KF(90/10) composite isothermally melt-crystallized at 96 and 100°C were observed by POM, and the results are shown in Figure 6. It is obviously observed that, with the addition of KF, the nucleation density increases significantly and the spherulite size drops drastically at both 96 and 100°C, confirming that KF can accelerate the nucleation of PBS. On the other hand, with increasing crystallization temperature, the nucleation density is reduced and the spherulite size increases.

The crystalline structure of the PBS and PBS/KF composites crystallized isothermally at 100°C, as well as the neat KF, was investigated with WAXD, as shown in Figure 7. The two peaks around $2\theta = 15.4°$ and $2\theta = 22.2°$, as shown in the KF sample, indicating that KF includes the cellulose crystal of type I, though the crystallinity seems to be relatively low.[27] The neat PBS and its composites all show strong reflections around $2\theta = 19.6°$ and 22.6°, because of the diffraction from (020) and (110) planes, respectively.[39] For these two peaks, no obvious change related to the diffraction peaks and peak position was observed with the increase of KF content, indicating that the crystalline structure of PBS is almost not affected by the addition of KF.

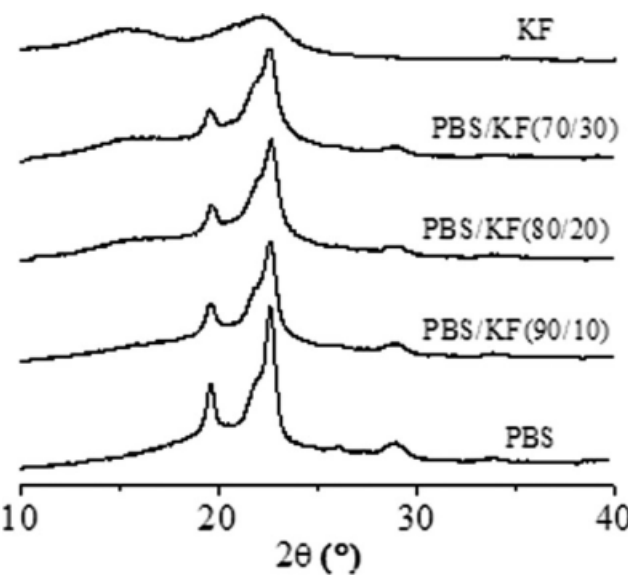

Figure 7 WAXD patterns of kenaf fiber, neat PBS, and PBS/KF composites. The PBS and its composites were prepared by isothermal melt-crystallization at 100°C.

CONCLUSIONS

In this study, the physical properties of the fabricated composites from untreated natural fiber KF reinforced PBS were investigated. Particularly, the effect of untreated KF on the mechanical properties and crystallization behavior of PBS in the composite were systematically studied. With the incorporation of KF, both the tensile modulus and the storage modulus are improved, and the crystallization rate of PBS is significantly enhanced. SEM analysis shows that the interfacial adhesion between PBS and KF needs further improvement. Future work will be focused on the improvements of the interfacial adhesion between KF and the polyester matrix and on the evaluation of the effect of KF on the biodegradability of polyester matrix in the composites.

References

1. Saheb, D. N.; Jog, J. P. Adv Polym Technol 1999, 18, 351.
2. Bledzki, A. K.; Gassan, J. Prog Polym Sci 1999, 24, 221.
3. Yu, L.; Dean, K.; Li, L. Prog Polym Sci 2006, 31, 576.
4. Mohanty, A. K.; Misra, M.; Hinrichsen, G. Macromol Mater Eng 2000, 276, 1.
5. Avella, M.; Casale, L.; dell'Erba, R.; Martuscelli, E. Macromol Symp 1998, 127, 211.
6. Nair, K. C. M.; Kumar, R. P.; Thomas, S.; Schit, S. C.; Ramanmurthy, K. Compos A 2000, 31, 1231.
7. Hepworth, D. G.; Vincent, J. F. V.; Jeronimidis, G.; Bruce, D. M. Compos A 2000, 31, 599.
8. Hill, C. A. S.; Khalil, H. P. S. J Appl Polym Sci 2000, 78, 1685.
9. Oksman, K. L.; Berglund, W. L. A. J Appl Polym Sci 2002, 84, 2358.
10. Stael, G. C.; Tavares, M. I. B. Polym Test 2000, 19, 251.
11. Pothan, L. A.; Oommen, Z.; Thomas, S. Compos Sci Technol 2003, 63, 283.
12. Rong, M. Z.; Zhang, M. Q.; Liu, Y.; Yang, G. C.; Zeng, H. M. Compos Sci Technol 2001, 61, 1437.
13. Sain, M. M.; Kokta, B. V. J Appl Polym Sci 1994, 54, 1545.
14. Sanadi, A. R.; Caufield, D. F.; Jacobson, R. E.; Rowell, R. M. Ind Eng Chem Res 1995, 34, 1889.
15. Lu, J. Z.; Wu, Q.; Negulescu, I. I. J Appl Polym Sci 2005, 96, 93.
16. Serizawa, S.; Inoue, K.; Iji, M. J Appl Polym Sci 2006, 100, 618.
17. Pan, P.; Zhu, B.; Kai, W.; Serizawa, S.; Iji, M.; Inoue, Y. J Appl Polym Sci 2007, 105, 1511.
18. Pan, P.; Zhu, B.; Dong, T.; Serizawa, S.; Iji, M.; Inoue, Y. J Appl Polym Sci 2008, 107, 3512.
19. Bhardwaj, R.; Monahty, A. K.; Drzal, L. T.; Pourboghrat, F.; Misra, M. Biomacromolecules 2006, 7, 2044.
20. Yang, A.; Wu, R. J Appl Polym Sci 2002, 84, 486.
21. Huda, M. S.; Drzal, L. T.; Misra, M.; Mohanty, A. K.; Williams, K.; Mielewski, D. F. Ind Eng Chem Res 2005, 44, 5593.
22. Huda, M. S.; Mohanty, A. K.; Drzal, L. T.; Schut, E.; Misra, M. J Mater Sci 2005, 40, 4221.
23. Keller, A. Compos Sci Technol 2003, 63, 1307.
24. Jiang, G.; Evans, M. E.; Jones, I. A.; Rudd, C. D.; Scotchford, C. A.; Walker, G. S. Biomaterials 2005, 26, 2281.
25. Shih, Y. F.; Lee, W. C.; Jeng, R. J.; Huang, C. M. J Appl Polym Sci 2006, 99, 188.
26. Shibata, M.; Ozawa, K.; Teramoto, N.; Yosomiya, R.; Takeishi, H. Macromol Mater Eng 2003, 288, 35.
27. Nishino, T.; Hirao, K.; Kotera, M.; Nakamae, K.; Inagaki, H. Compos Sci Technol 2003, 63, 1281.
28. Kori, Y.; Kitagawa, K.; Hamada, H. J Appl Polym Sci 2005, 98, 603.
29. Zini, E.; Focarete, L. M.; Noda, I.; Scandola, M. Compos Sci Technol 2007, 67, 2085.
30. Bikiaris, D. N.; Papageorgiou, G. Z.; Achilias, D. S. Polym Degrad Stab 2006, 91, 31.
31. Bleach, N. C.; Nazhat, S. N.; Tanner, K. E.; Kellomaki, M.; Tormala, P. Biomaterials 2002, 23, 1579.
32. Fay, J. J.; Murphy, C. J.; Thomas, D. A.; Sperling, L. H. Polym Eng Sci 1991, 31, 1731.
33. Dong, T.; He, Y.; Zhu, B.; Shin, K. M.; Inoue, Y. Macromolecules 2005, 38, 7736.
34. Miyata, T.; Masuko, T. Polymer 1998, 39, 1399.
35. Gan, Z.; Abe, H.; Dio, Y. Biomacromolecules 2001, 2, 313.
36. Albano, C.; Papa, J.; Ichazo, M.; Gonzalez, J.; Ustariz, C. Compos Struct 2003, 62, 291.
37. Avrami, M. J Chem Phys 1939, 7, 1103.
38. Avrami, M. J Chem Phys 1941, 9, 177.
39. Ichikawa, Y.; Kondo, H.; Igarashi, Y.; Noguchi, K.; Okuyama, K.; Washiyama, J. Polymer 2000, 41, 4719.